First-principles study of surface segregation in Cu-Ni alloys

A. Pasturel
Laboratoire de Thermodynamique et Physico-Chimie Metallurgiques, Domaine Universitaire, 38402 Saint Martin d'Hères, France

V. Drchal
Institute of Physics, Czechoslovak Academy of Sciences, CS-180 40 Praha 8, Czechoslovakia

J. Kudrnovský
Institute of Physics, Czechoslovak Academy of Sciences, CS-180 40 Praha 8, Czechoslovakia and Institut für Technische Elektrochemie, Technische Universität, A-1060 Wien, Austria

P. Weinberger
Institut für Technische Elektrochemie, Technische Universität, A-1060 Wien, Austria
(Received 23 November 1992)

A method coupling electronic structure calculations with Monte Carlo simulations has been developed to determine surface compositions in Cu-Ni alloys. The calculations are based on an effective Ising model with parameters as defined within the framework of the generalized perturbation method and as calculated by means of the tight-binding version of the linear-muffin-tin-orbital method. Properties of Cu-Ni bulk alloys are discussed in terms of bulk effective interatomic interactions. The composition profiles are obtained for the fcc (001) surface for three bulk compositions, namely, $Cu_{75}Ni_{25}$, $Cu_{50}Ni_{50}$, and $Cu_{25}Ni_{75}$. The major role played by the layer-dependent site-diagonal terms in the Ising model is emphasized. Our results are found to be in agreement with available experimental data.

I. INTRODUCTION

In view of the technological importance of metallic alloy surfaces for catalysis[1] and problems of corrosion,[2] the phenomenon of surface segregation has been the subject of many theoretical[3–9] and experimental[10–16] studies. Qualitatively, surface enrichment and the expected ordering or clustering can be understood in terms of the variations in the electronic structure upon alloying and the presence of an abrupt boundary, in terms of which the surface has to be viewed. For bulk solids, ordering and clustering phenomena are currently studied within a microscopic theory based on a generalized three-dimensional (3D) Ising model.[17] Two types of approaches have been developed to calculate the parameters entering the 3D Ising model. The first one is the so-called Connolly-Williams inversion[18] and the closely related renormalized interaction method.[19] These methods use standard *ab initio* band-structure techniques as applied to a suitably chosen set of periodic crystal structures, whose total energies are mapped onto the parameters of the Ising model. In the second approach, the energy of the completely disordered state as calculated by means of the coherent potential approximation[20] (CPA) is the starting point. The Ising model parameters or effective cluster interactions are then calculated using the embedded cluster method[21] or the generalized perturbation method (GPM),[22,17] whereby the explicit expressions for cluster interactions provide a physical insight into the problem of ordering.[23,24]

Only recently attempts were made to generalize the GPM theory also to the case of alloy surfaces. In the very first studies an empirical tight-binding model was applied[25] which used the recursion method[26] and described the semi-infinite solids by a finite cluster. Recently a method[27] for the calculation of the parameters for the 3D Ising model for semi-infinite disordered alloys within the GPM approach, based on the first-principles tight-binding linear-muffin-tin-orbital (TB-LMTO) method,[28] was developed. The first application of this method was the explanation of the origin of the formation of ordered surface alloys on clean transition metal surfaces.[29] In this paper segregation phenomena, namely the enrichment of the surface layer by one of the alloy components, are studied. In order to determine the surface concentration and the concentration profile, a multilayer treatment of surface segregation is required. This can be achieved by using mean-field approximations such as the Bragg-Williams approximation[3–5] or more accurately the cluster variation method[8,9] or Monte Carlo simulations.[6,7] In the present paper Monte Carlo simulations are performed to study the surface segregation in Cu-Ni alloys. The paper is organized as follows. In Sec. II we summarize the essential features of the 3D Ising model for a semi-infinite disordered alloy. In Sec. III follows a discussion of the applied Monte Carlo simulation technique. The predictions of the method for the thermodynamics of bulk Cu-Ni alloys are presented in Sec. III A, while in Sec. III B the surface composition profiles of the fcc (001) face of Cu-Ni alloys as a function of the

bulk concentration are given and compared with available experimental results.

II. FORMALISM

The method of how to describe the electronic structure of a semi-infinite disordered alloy with concentration inhomogeneities near the surface was described in detail elsewhere.[30,31] Here we just summarize its basic features. The alloy disorder is included via the CPA generalized to inhomogeneous systems with only two-dimensional translational symmetry using the first-principles TB-LMTO method. Due to the semi-infinite nature of the problem, in principle all layers can have different physical properties. In order to overcome this difficulty, we assume that from a certain layer on, the electronic properties of all subsequent layers are identical to those of the corresponding infinite systems, namely either to a homogeneous alloy or to the vacuum. The semi-infinite alloy is thus considered to be divided into three regions: (i) a homogeneous bulk alloy, (ii) a homogeneous vacuum region represented by empty spheres and characterized by flat potentials, and (iii) an intermediate region consisting of several (M) atomic layers, where all inhomogeneities (chemical or electronic) are located, and which contains also a few layers of empty spheres of the vacuum-solid interface. The combined effect of alloy disorder and of the semi-infinite geometry requires the use of a surface Green's-function formalism.[30–32]

The Green's function $g(z) = [P(z) - S]^{-1}$ is defined in terms of the potential function matrix $P(z)$ and the structure constants matrix S. The potential functions, which characterize the scattering properties of individual sites at positions $\mathbf{R}$, are random but site-diagonal quantities. The structure constants S, which describe the intralayers and interlayers coupling, are nonrandom site off-diagonal quantities. In the so-called tight-binding muffin-tin-orbital representation[2,7] the interatomic coupling is extremely short ranged, which greatly simplifies the theoretical treatment.

The semi-infinite homogeneous alloy or the vacuum can be represented by a single quantity, the surface Green's function (SGF) by which the problem of an infinite number of layers can be reduced to a problem of a finite number of layers, namely to the intermediate region. The SGF, the central quantity of the present formalism, can be calculated effectively by means of short-ranged structure constants.[32]

The site off-diagonal elements of the configurationally averaged Green's function within a given layer as well as in between different layers essentially determine the parameters of the Ising model

$$H^I = E_0 + \sum_{\mathbf{R}} \sum_{\alpha} D^{\alpha}_{\mathbf{R}} \eta^{\alpha}_{\mathbf{R}} + \frac{1}{2} \sum_{\mathbf{R},\mathbf{R}'} \sum_{\alpha,\alpha'} V^{\alpha,\alpha'}_{\mathbf{R},\mathbf{R}'} \eta^{\alpha}_{\mathbf{R}} \eta^{\alpha'}_{\mathbf{R}'} + \cdots \quad (\alpha, \alpha' = A, B), \tag{1}$$

where E_0 is the configurationally independent part of the alloy internal energy, $D^{\alpha}_{\mathbf{R}}$ is the on-site energy, and $V^{\alpha,\alpha'}_{\mathbf{R},\mathbf{R}'}$ are the pair interatomic interactions.

A particular configuration of the alloy is characterized by a set of occupation indices $\eta^{\alpha}_{\mathbf{R}}$, where $\eta^{\alpha}_{\mathbf{R}} = 1$ if site $\mathbf{R}$ is occupied by an atom of type α, and $\eta^{\alpha}_{\mathbf{R}} = 0$ otherwise. The parameters of the Ising model are found within the GPM by mapping at $T = 0$ the grand canonical potential $\Omega_{\rm el}(T = 0, E_F)$ of the electronic subsystem (where E_F is the Fermi energy),

$$\Omega_{\rm el}(T = 0, E_F) = -\int_{-\infty}^{E_F} N(E)\, dE, \tag{2}$$

onto the Hamiltonian in Eq. (1). The integrated density of states $N(E)$ for a particular configuration of the alloy within the TB-LMTO-CPA formalism is given by the expression[27]

$$N(E) = -\frac{1}{\pi} \lim_{\delta \to 0^+} \mathrm{Im\,Tr} \left\{ \frac{1}{2} \ln \left[\frac{d}{dz} P(z) \right] + \ln g(z) \right\} \quad (z = E - i\delta), \tag{3}$$

where the first term compensates the extra singularities in $\ln g(z)$ which originate from the poles of $P(z)$. By decomposing the Green's function $g(z)$ into its diagonal and off-diagonal parts with respect to lattice sites, the usual GPM expansion of Eq. (3) yields for the Ising Hamiltonian parameters the following expressions:

$$D^{\alpha}_{\mathbf{R}} = \frac{1}{\pi} \mathrm{Im\ tr} \int_{-\infty}^{E_F} \left(\lim_{\delta \to 0^+} \ln \{ 1 + [P^{\alpha}_{\mathbf{R}}(z) - \mathcal{P}_{\mathbf{R}}(z)]\, \bar{g}_{\mathbf{RR}}(z) \} \right) dE, \tag{4}$$

and

$$V^{\alpha\alpha'}_{\mathbf{RR}'} = \frac{1}{\pi} \mathrm{Im\ tr} \int_{-\infty}^{E_F} \left(\lim_{\delta \to 0^+} \ln [1 - t^{\alpha}_{\mathbf{R}}(z)\, \bar{g}_{\mathbf{RR}'}(z)\, t^{\alpha'}_{\mathbf{R}'}(z)\, \bar{g}_{\mathbf{R}'\mathbf{R}}(z)] \right) dE. \tag{5}$$

In Eqs. (3)–(5), Tr denotes the trace in configurational and angular momentum space, while tr means the trace over the angular momentum space only. The quantity $\bar{g}_{\mathbf{RR}'}(z)$ is the configurationally averaged Green's function between the sites $\mathbf{R}$ and $\mathbf{R}'$, which in general belong to different layers. For a particular site $\mathbf{R}$ in a given layer p, $t^{\alpha}_{\mathbf{R}}(z)$ is the on-site element of the single-site t matrix. The quantity $\mathcal{P}_{\mathbf{R}}(z)$ is the (nonrandom) configurationally averaged coherent potential function, which is site diagonal. The coherent potential function

$$\mathcal{P}_{\mathbf{R}}(z) = \begin{cases} \mathcal{P}_p(z),\ p = 1, 2, \ldots M & \text{in the intermediate region} \\ P^b(z) \text{ or } P^v(z) & \text{otherwise,} \end{cases} \tag{6}$$

has in general different values for the layers in the intermediate region. In (6) indices b and v refer to the bulk alloy and the vacuum region, respectively. In the intermediate region ($1 \leq p \leq M$) the coherent potential functions $\mathcal{P}_p(z)$ are found from a set of coupled inhomogeneous CPA equations.[30,31]

In principle, one can start from the inhomogeneous reference medium $\mathcal{P}_p(z)$ as defined by Eq. (6), and vary then the concentration profile according to the Monte Carlo simulation. In this manner, complete consistency between the reference medium and the Monte Carlo simulations can be achieved. This approach will be the subject of the forthcoming study. Here we limit ourselves to the simple but plausible case, when the reference medium refers to a homogeneous bulk alloy, i.e., where $\mathcal{P}_p(z) = \mathcal{P}^b(z)$ for each layer p in the intermediate region and where $\mathcal{P}^b(z)$ is found from charge self-consistent TB-LMTO-CPA calculations for the bulk alloy. This description is along the lines of the tight-binding Ising model approach[25,17] developed by Treglia and co-workers.

Using the transformation to the lattice gas model, $\eta^A_{\mathbf{R}} = 1 - \eta^B_{\mathbf{R}} \equiv \eta_{\mathbf{R}}$, and limiting the expansion to single-site and pair interactions, the Ising Hamiltonian less a constant [see Eq. (1)] can be written as

$$H^I = \sum_{\mathbf{R}} \mathcal{D}_{\mathbf{R}} \eta_{\mathbf{R}} + \frac{1}{2} \sum_{\mathbf{R},\mathbf{R}'} \mathcal{V}_{\mathbf{R},\mathbf{R}'} \eta_{\mathbf{R}} \eta_{\mathbf{R}'}, \tag{7}$$

where

$$\mathcal{D}_{\mathbf{R}} = D^A_{\mathbf{R}} - D^B_{\mathbf{R}} + \sum_{\mathbf{R}' \neq \mathbf{R}} [\, V^{AB}_{\mathbf{R}\mathbf{R}'} - V^{BB}_{\mathbf{R}\mathbf{R}'}], \tag{8}$$

$$\mathcal{V}_{\mathbf{R}\mathbf{R}'} = V^{AA}_{\mathbf{R}\mathbf{R}'} + V^{BB}_{\mathbf{R}\mathbf{R}'} - V^{AB}_{\mathbf{R}\mathbf{R}'} - V^{BA}_{\mathbf{R}\mathbf{R}'} . \tag{9}$$

The quantities $\mathcal{V}_{\mathbf{R}\mathbf{R}'}$ are the so-called renormalized effective pair interactions (REPI). The unrenormalized effective pair interactions (EPI) correspond to the first-order expansion of the logarithm in Eq. (5). In a similar way, triplet and higher multisite interactions can be defined.[21,27] The quantity $\mathcal{D}_{\mathbf{R}}$ is the renormalized effective level or point-cluster energy, which contributes significantly to segregating processes in inhomogeneous systems.

III. MONTE CARLO CALCULATIONS

Once the effective Ising model has been defined, thermodynamic theories such as a mean-field Bragg-Williams approximation, the cluster variation method, or the Monte Carlo simulation technique can be applied. Minimizing the resulting free energy with respect to the concentrations in the various layers under the constraint of a fixed bulk concentration leads in the Bragg-Williams approximation to a set of coupled equations for the layer-dependent concentrations. Such equations have been used by several authors;[3,4,25,26] however, improvements in the free-energy minimization scheme, based on the cluster variation method[8,9] or the Monte Carlo method,[6,7] are now straightforward and permit the calculation of the short-range ordering within the surface layers below the bulk disordering temperatures.

The present Monte Carlo simulations do not include displacements from the positions of the two-dimensional coherent lattice. In order to reduce the numerical effort, a three-dimensional fcc rigid lattice is simulated with a finite number of atoms. Periodic boundary conditions are imposed in two directions parallel to the surface. In general the number of atomic layers in each computational cell depends on the crystal face. For the fcc (001) surface we have used eight layers each containing $N_p = 15 \times 17$ atoms (the total number of atoms in the computational cell in $N = 8 \times N_p$). A few simulations with thicker slabs or larger surface areas were performed and the resulting surface compositions proved to be the same as for the above size. The simulation proceeds as follows. The starting configuration $C^{(1)}$ is constructed in a random way with respect to the bulk composition. In a repetitive manner, we first pick randomly an atom in a given configuration $C^{(n)}$ and select, again randomly, one of its nearest neighbors. Secondly, we study the variation of the total energy of the system, ΔE, due to the interchange of these two atoms. Two cases are possible according to the sign of ΔE, namely, (i) $\Delta E < 0$: the interchange of two atoms is energetically favorable and represents the new configuration $C^{(n+1)}$; and (ii) $\Delta E \geq 0$: the interchange is not necessarily energetically favorable. The two atoms are only interchanged to form a new configuration $C^{(n+1)}$ if $\exp(-\Delta E/kT) > \tau$, where τ is a random number ($\tau \in [0,1]$).

This procedure is repeated by choosing a new central atom and the system approaches the thermodynamical equilibrium if the number of interchanges is sufficiently large. The two planes furthest from the surface serve as a reservoir of atoms having the average bulk composition. To determine the equilibrium, the average value of a thermodynamical property is generally not sufficient and an error estimation, like a standard deviation, must be provided. In order to avoid correlations in the various steps of the Markov chain[7] the output parameters can be defined as

$$\langle c_p \rangle = \frac{1}{m} \sum_{j=\mu_0}^{\mu_0+m} c_p(\nu_j), \tag{10}$$

where c_p is the concentration of A atoms in the pth plane, and $\nu_j = jN$, N is the number of atoms in the computational cell.

The value of μ_0 must be large enough to eliminate the influence of the initial configuration and m, the number of iterations, is chosen as large as possible to reduce the standard deviation defined as

$$(\Delta c_p)^2 = \frac{1}{m(m-1)} \sum_{j=\mu_0}^{\mu_0+m} [c_p(\nu_j) - \langle c_p \rangle]^2 . \tag{11}$$

The values used for the present results are $m = 200N$ and $\mu_0 = 80N$. It should be noted that this choice of computational parameters depends on the temperature at which the simulation is performed, whereby near the critical temperature these values have to be substantially increased.

A. Bulk Cu-Ni alloys

In the past, the Cu-Ni system was very often considered to be a classical example for a substitutional solid solution since it seemed to exhibit complete miscibility over the whole range of concentrations, and also since Cu and Ni differ little in their atomic volumes. It has been shown experimentally,[33] however, that Cu-Ni alloys in fact tend to phase separate at temperatures below 700 K and also for high Ni concentrations. The latest assessment of the Cu-Ni phase diagram[34] places the critical point of the miscibility gap at 65.6% Ni and 627.5 K. In particular interest for our study is the analysis of the experimental neutron scattering data in Cu-Ni alloys[35] by means of the cluster field method (CFM),[36] which showed that the first and second nearest-neighbor (NN) pair interactions have about the same amplitude but are of opposite signs with the first NN pairs being negative. Morever, the CFM interactions exhibit a strong variation with composition with a distinct maximum occurring at about 60% of Cu atoms. From the theoretical point of view, the Cu-Ni system has several attractive features: the elastic contributions are small and so are the relativistic effects for the valence-band structure. In addition, magnetic interactions are negligible at least for Cu-rich compositions. Because of the available experimental evidence, we have also calculated the effective cluster interactions for the bulk alloys $Cu_{25}Ni_{75}$, $Cu_{50}Ni_{50}$, and $Cu_{75}Ni_{25}$. In these calculations the maximum angular momentum was restricted to two and the atomic sphere radii of alloy components were chosen such that these spheres are approximately charge neutral. The Brillouin zone (BZ) integrations were carried out over the full BZ (2048 $\mathbf{k}$ points). All calculations are performed in the complex energy plane and then analytically continued to the real axis. In accordance with the experimental lattice constants,[34] the alloy lattice parameters are linearly interpolated between the equilibrium lattice parameters of pure elements.

We found that both the REPI's and EPI's for Cu-Ni alloys are in very good quantitative agreement with each other. In Table I, the EPI's are compared with the CFM interactions. As one can see, the first and second pair interactions indeed have about the same amplitude but opposite signs just as the CFM interactions. However, the first NN interactions are more negative on the Ni-rich side than on the Cu-rich side, which contradicts the CFM results, but is in agreement with those experimental data[33,34] that locate the miscibility gap towards the Ni-rich side. The maximum for the CFM interactions at about 60% of Cu atoms has been interpreted in terms of the crossing of the d-band edge by the Fermi level. However, the consequences for the pair interactions are far from being obvious.[37] As in the CFM we also find that the more distant interactions are negligible. It can be stated therefore that the bulk EPI's as obtained by our TB-LMTO-GPM calculations appear to be quite reasonable. A calculation of the bulk phase diagram based on these parameters will be presented elsewhere.

B. fcc (001) Cu-Ni alloy surfaces

The surface segregation in Cu-Ni alloys has been the subject of intense theoretical[3–9] and experimental[10–16] studies. It is now agreed that Cu segregates to the surface upon annealing in the temperature range of about 600–900 K, even at the Ni-rich end for which the situation seemed to be controversial,[14,15] whereby the Cu segregation is not sensitive to orientation of the surface. In the present paper the (001) face of the fcc alloys $Cu_{25}Ni_{75}$, $Cu_{50}Ni_{50}$, and $Cu_{75}Ni_{25}$ is considered. The BZ integrations were performed over the full surface BZ using 400 $\mathbf{k}_{\|}$ points. All Monte Carlo simulations have been performed at 800 K. This temperature is within the range of temperatures at which various experimental studies were performed.[10–16] For the vacuum-solid interface a hard-wall-like boundary condition was assumed. We also performed calculations corresponding to an imagelike barrier as derived from self-consistent surface calculations.[31] The corresponding results for the Cu-Ni system indicate that the Ising model parameters are not very sensitive to the actual form of the surface barrier.

We have calculated all REPI's up to the distance of fourth NN in an fcc lattice within a given layer as well as in between various layers near the surface. Due to the fast convergence of the layer Green's functions to the bulk Green's function, one can identify[27] the first, second, and fourth NN REPI's in the fourth layer, and

TABLE I. Comparison between CFM effective pair interactions (Ref. 36) and calculated GPM effective pair interactions as a function of the Cu concentration. The values V_1, V_2, and V_3 refer to first, second, and third nearest-neighbor pair interactions. All values are in mRy per atom.

c^{Cu}	V_1^{CFM}	V_2^{CFM}	V_3^{CFM}	V_1^{GPM}	V_2^{GPM}	V_3^{GPM}
20	-1.86	1.67	-0.47			
25				-1.37	0.51	0.00
30	-1.72	1.33	-0.01			
44	-1.77	0.96	-0.02			
50				-0.96	1.10	0.08
52	-1.63	1.13	-0.62			
60	-2.25	3.96	-0.88			
70	-2.37	3.38	-0.64			
75				-0.45	1.06	0.28

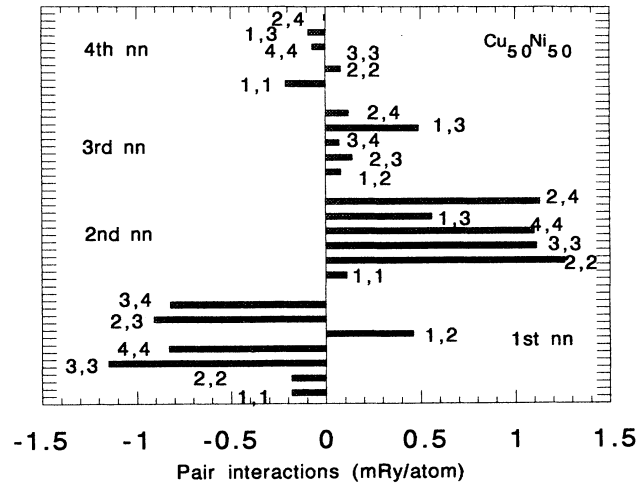

FIG. 1. Renormalized effective pair interactions for the (001) face of $Cu_{50}Ni_{50}$. The positions of atoms forming a pair are specified by the layer indices p, q (index 1 refers to the surface) and by the type of neighbors (first to fourth nearest neighbors).

the third NN REPI's between the third and fourth layers with the corresponding bulk values.

The REPI's for the (001) surface of $Cu_{50}Ni_{50}$, presented in Fig. 1, show a fast decrease with distance in all layers including the surface layer. Note that contrary to qualitative conclusions made on the basis of a simple empirical tight-binding model,[25] the first NN surface REPI just like for Pd-Rh and Ag-Pd systems[27] is not dominating. The values of the effective triplet interactions are generally small compared to the REPI's, which in turn simplifies considerably Monte Carlo studies. The values of the point-cluster energies are often considered to be decisive for the segregating phenomena at the alloy surfaces.[25] In Fig. 2 the difference $(D_p - D_b)$ between the point-cluster energies in the pth atomic layer in the intermediate region and the bulk layer is shown. We found a quick convergence of these on-site energies to the bulk value, but the most important result is that the difference at the surface layer is large as compared to the REPI's values. This result confirms the decisive role played by these quantities in the segregation process. Another important feature is a weak concentration dependence of the $(D_p - D_b)$ values. Roughly speaking, as shown in Ref. 25, this difference is proportional to the difference in the surface tension of the pure constituents. All these facts allow one to simplify further the Monte Carlo calculations. As mentioned in Sec. II, in a proper treatment of the segregation process, both the REPI's and the point-cluster energies, and the concentration profiles should be determined in a self-consistent manner. Because the REPI values are an order of magnitude smaller than the point-cluster energies, their concentration dependence can be neglected. To confirm this assumption, in Fig. 3 the concentration profile of the (001) surface

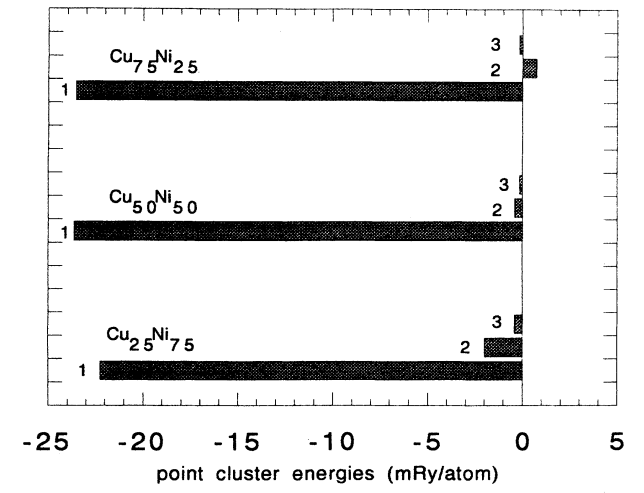

FIG. 2. The difference $(D_p - D_b)$ of the point-cluster energies between the pth atomic layer (index 1 refers to the surface) and the bulk layer b for fcc (001) Cu-Ni alloys.

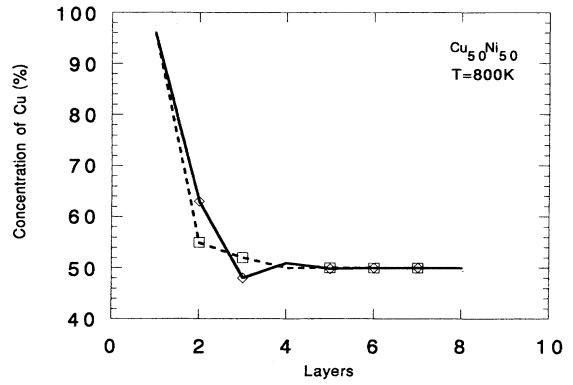

FIG. 3. The Cu concentration profile for fcc (001)-$Cu_{50}Ni_{50}$ vs the layer index as obtained from the Monte Carlo calculations. Layer 1 corresponds to the surface while the concentrations in layers 7 and 8 were kept frozen to the bulk concentration: point-cluster and pair interactions (full line); point-cluster interactions only (dashed line).

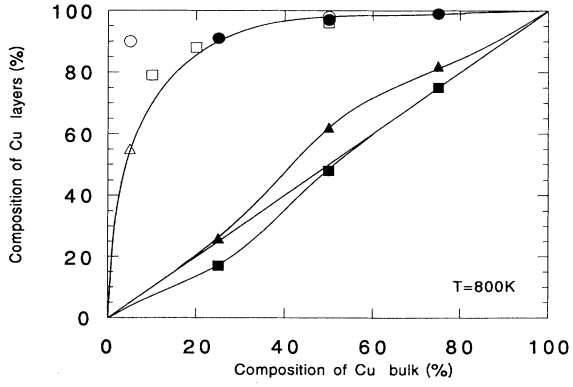

FIG. 4. The surface compositions vs bulk composition for fcc (001) Cu-Ni alloys at T=800 K: (•) surface layer; (▲) second sample layer; (■) third sample layer. Experimental results: (○) Ref. 16, T=880 K; (△) Ref. 13, T=823 K; (□) Ref. 12, T=773 K. The lines shown serve as a guide for the eye.

of $Cu_{50}Ni_{50}$ is shown with and without the contribution from the pair interactions. One can see that the concentration profiles are quite similar, emphasizing the role played by the point-cluster energies. Both calculations predict a strong Cu segregation but they show small differences in the shape of the segregation profile. A strong correlation between the $(D_p - D_b)$ values and the segregation process is noticeable: the segregation is large for layers where the differences $(D_p - D_b)$ are large as compared to the REPI's. The values of $(D_p - D_b)$ quickly approach zero deeper inside the bulk where the concentration profile approaches the bulk concentration.

The calculated concentrations in the first three layers of the (001) surfaces for the above three alloys are plotted as a function of the bulk concentration in Fig. 4 and compared with available experimental data. Our results are in a very good quantitative agreement with most experimental results, which all show a strong Cu segregation at the surface, independent of the bulk composition and the surface orientation. Our results do not indicate the possibility of a crossover of the surface segregation to Ni enrichment at Cu composition higher than 80% as obtained by the time of flight atom probe measurements.[15]

IV. CONCLUSIONS

We have performed calculations for the segregation in Cu-Ni alloys using the Monte Carlo simulation technique for a 3D Ising model for which the TB-LMTO-GPM technique has been used to evaluate the layer- and concentration-dependent effective levels and effective cluster interactions. The Monte Carlo simulations indicate the crucial importance of the on-site terms in the Ising model for the segregation process. For the Cu-Ni system, we found that starting from Ising model parameters corresponding to the homogeneous reference medium (bulk compositions in all layers including the surface) the results are in very good agreement with available experimental data.

The present version of the theory can be generalized by including the effect of layer relaxations at the surface, or by taking into account relativistic effects. It can be used to clarify even more subtle effects of surface segregation such as the anisotropy in the Cu-Pt alloys[38] with respect to different orientations of the surface. This anisotropy could be a consequence of a strong competition between surface segregation and bulk ordering tendencies. Yet another interesting application concerns the problem of the surface-induced ordering or disordering[39] in the fcc-binary alloys.

ACKNOWLEDGMENTS

This paper was supported by the Czechoslovak Academy of Sciences (Project No. 11015), the Austrian Ministery of Science (Project No. GZ 45.123./1-II/A/4/91), and the Austrian Science Foundation (Grant No. P8918).

[1] J.W. Gibbs, *The Collected Works of J.W. Gibbs* (Yale University Press, New Haven, 1948), Vol. 1.
[2] D. McLean, *Grain Boundaries in Metals* (Oxford University Press, London, 1981).
[3] F.L. Williams and D. Nason, Surf. Sci. **45**, 377 (1974).
[4] D. Kumar, A. Mookerjee, and V. Kumar, J. Phys. F **6**, 725 (1976).
[5] G. Treglia and B. Legrand, Phys. Rev. B **35**, 4338 (1987).
[6] R.G. Donnelly and T.S. King, Surf. Sci. **74**, 89 (1978).
[7] J. Eymery and J.C. Joud, Surf. Sci. **231**, 419 (1990).
[8] V. Kumar and K.H. Bennemann, Phys. Rev. Lett. **53**, 278 (1984).
[9] J.M. Sanchez and J.L. Moran-Lopez, Phys. Rev. B **32**, 3534 (1985).
[10] J.M. Sinfelt, J.L. Carter, and D.J. Yates, J. Catalys. **24**, 280 (1972).
[11] K. Watanabe, M. Hashida, and T. Yamashina, Surf. Sci. **61**, 483 (1976).
[12] H.H. Brongersma, M.J. Sparnaay, and T.M. Buck, Surf. Sci. **71**, 657 (1978).
[13] Y.S. Ng, T.T. Tsong, and S.B. McLane, Jr., Phys. Rev. Lett. **42**, 588 (1979).
[14] H.H. Brongersma, P.A.J. Ackermans, and A.D. van Langeveld, Phys. Rev. B **34**, 5974 (1986).
[15] T. Sakurai, T. Hashizume, A. Jimbo, A. Sakai, and S. Hyodo, Phys. Rev. Lett. **55**, 514 (1985).
[16] R. Weber, C.E. Rojas, P.J. Dobson, and D. Chadwick, Surf. Sci. **105**, 20 (1981).
[17] F. Ducastelle, *Order and Phase Stability* (North-Holland, Amsterdam, 1991).
[18] J.W. Connolly and A.R. Williams, Phys. Rev. B **27**, 5169 (1983).
[19] S.H. Wei, L.G. Ferreira, and A. Zunger, Phys. Rev. B **41**, 8240 (1990); Z.W. Lu, S.H. Wei, and A. Zunger, Phys. Rev. Lett. **66**, 1753 (1991).
[20] B. Velický, S. Kirkpatrick, and H. Ehrenreich, Phys. Rev. **175**, 747 (1968).
[21] A. Gonis, X.G. Zhang, A.J. Freeman, P. Turchi, G.M. Stocks, and D.M. Nicholson, Phys. Rev. B **36**, 4630 (1987).
[22] F. Ducastelle and F. Gautier, J. Phys. F **6**, 2039 (1976).
[23] P. Turchi, G.M. Stocks, W.H. Butler, D.M. Nicholson, and A. Gonis, Phys. Rev. B **37**, 5982 (1988).
[24] L. Szunyogh and P. Weinberger, Phys. Rev. B **43**, 3768 (1991).
[25] B. Legrand, G. Treglia, and F. Ducastelle, Phys. Rev. B **41**, 4422 (1990); G. Treglia, B. Legrand, and F. Ducastelle, Europhys. Lett. **7**, 575 (1988).
[26] H. Dreyssé, L.T. Wille, and D. de Fontaine, Solid State Commun. **78**, 355 (1991).
[27] V. Drchal, J. Kudrnovský, L. Udvardi, P. Weinberger, and A. Pasturel, Phys. Rev. B **45**, 14 328 (1992).
[28] O.K. Andersen and O. Jepsen, Phys. Rev. Lett. **53**, 2571 (1984).
[29] J. Kudrnovský, S.K. Bose, and V. Drchal, Phys. Rev. Lett. **69**, 308 (1992).
[30] J. Kudrnovský, P. Weinberger, and V. Drchal, Phys. Rev. B **44**, 6410 (1991).
[31] J. Kudrnovský, I. Turek, V. Drchal, P. Weinberger, S.K. Bose, and A. Pasturel, Phys. Rev. B. **47**, 16 525 (1993).
[32] B. Wenzien, J. Kudrnovský, V. Drchal, and M. Šob, J.

Phys. Condens. Matter **1**, 9893 (1989).
[33]S. An Mey, Z. Metall. **78**, 502 (1987).
[34]*Binary Alloy Phase Diagrams*, edited by T.B. Massalski, 2nd ed. (ASM International, Metals Park, Ohio, 1990).
[35]J. Vrijen and S. Radelaar, Phys. Rev. B **17**, 409 (1978).
[36]V.G. Vaks, N.E. Zein, and V.V. Kamyshenko, J. Phys. Condens. Matter **1**, 2115 (1989).
[37]M. Sluiter and P.E.A. Turchi, in *Alloy Phase Stability and Design*, edited by G.M. Stocks, D.P. Pope, and A.F. Giamei, MRS Symposia Proceedings No. 186 (Materials Research Society, Pittsburgh, 1991), p. 77.
[38]F. Ducastelle, B. Legrand, and G. Treglia, Prog. Theor. Phys. (Suppl.) **101**, 159 (1990).
[39]W. Schwejka, K. Binder, and D.P. Landau, Phys. Rev. Lett. **65**, 3321 (1990).